

Multi-omics approach to improve patient-tailored therapy using immune checkpoint blockade and cytokine-induced killer cell infusion in an elderly patient with lung cancer: A case report and literature review

YASI XING¹, FANGYUAN QIN¹, LEI HAN¹, JINGWEN YANG¹, HONGRUI ZHANG²,
YONG QI³, SHICHUN TU^{2,4} and YAPING ZHAI¹

¹Henan Eye Institute, Henan Eye Hospital, Henan Provincial People's Hospital; ²Zhengzhou Shenyou Biotechnology;

³Department of Respiratory and Critical Care Medicine, Henan Provincial People's Hospital, People's Hospital of Zhengzhou University, Zhengzhou, Henan 450001, P.R. China;

⁴Scintillon Institute for Biomedical and Bioenergy Research, San Diego, CA 92121, USA

Received August 9, 2023; Accepted February 6, 2024

DOI: 10.3892/ol.2024.14334

Abstract. The 5-year survival rate of patients with advanced non-small cell lung cancer (NSCLC) remains low, despite recent advances in targeted therapy and immunotherapy. Therefore, there is a need to identify alternative strategies to improve treatment outcomes. Modern diagnostics can significantly facilitate the selection of treatment plans to improve patient outcomes. In the present study, multi-form diagnostic methodologies were adopted, including next-generation sequencing-based actionable gene sequencing, programmed death ligand 1 (PD-L1) immunohistochemistry, a circulating tumor cell (CTC) assay, flow cytometric analysis of lymphocyte subsets and computed tomography, to improve disease management in an 86-year-old female patient with relapsed metastatic NSCLC. High expression of PD-L1, elevated CTC mutations, were observed. Based on these results, the patient

was initially treated with the programmed death protein 1 blocking antibody sintilimab for two cycles, resulting in the stabilization of their condition, although the patient still exhibited severe pain and other symptoms, including fatigue, malaise, a loss of appetite and poor mental state. Informed by dynamic monitoring of the patient's response to treatment, the treatment plan was subsequently adjusted to a combination therapy with sintilimab and autologous cytokine-induced killer cell infusion, which eventually led to improved outcomes in both the management of the cancer and quality of life. In conclusion, multi-omics analysis may be used to establish patient-tailored therapies to improve clinical outcomes in hard-to-treat elderly patients with metastatic NSCLC.

Introduction

Non-small-cell lung cancer (NSCLC) is the leading cause of cancer-associated mortality in China and worldwide (1-3). Although significant improvements have been achieved due to the development of targeted therapies, the 5-year survival rate remains low (4), particularly in elderly patients with refractory/relapsed (R/R) disease who are often unsuitable for most conventional treatments, including surgery and chemotherapy (5). Immunotherapy with programmed death protein 1 (PD-1)/programmed death ligand 1 (PD-L1) blocking antibodies has shown significant promise in treating patients with R/R diseases (6,7). However, this benefit was only found in a small subset of the patient population (8), thus highlighting the need for alternative approaches to improve outcomes. The availability of multi-form diagnostic platforms can be used to provide additional information to improve decision-making regarding treatments, with the aim of leading to improved remission.

Combination therapies, including those based on PD-1 blockade, have significantly improved treatment outcomes and response rates in patients with cancer (9,10). It has been reported that PD-1 blockade can be potentiated by cytokine-induced

Correspondence to: Professor Yaping Zhai, Henan Eye Institute, Henan Eye Hospital, Henan Provincial People's Hospital, 7 Weiwu Road, Jinshui, Zhengzhou, Henan 450001, P.R. China
E-mail: ypzhai0000@163.com

Professor Shichun Tu, Scintillon Institute for Biomedical and Bioenergy Research, 6888 Nancy Ridge Drive, San Diego, CA 92121, USA
E-mail: shichuntu@scintillon.org

Abbreviations: NSCLC, non-small cell lung cancer; PD-1, programmed death protein 1; PD-L1, programmed death ligand 1; NGS, next-generation sequencing; CTC, circulating tumor cell; CIK, cytokine-induced killer; IHC, immunohistochemistry; SD, stable disease; CR, complete response; PR, partial response; NK, natural killer

Key words: multi-omics, PD-1 blockade, CIK cells, NSCLC, combination therapy, immunotherapy

killer (CIK) cell infusion (11-16), and a combination of these two types of treatments has been trialed in advanced NSCLC where it has demonstrated improved outcomes (16-18). CIK cells are a group of heterogeneous and major histocompatibility complex-unrestricted cells with a mixed T/natural killer (NK) phenotype (19,20). Compared with CAR-T cell therapy, which is only effective in hematological malignancies, CIK therapy can be effective in the treatment of both hematological and solid malignancies with low toxicity (16-18,21-23).

In the present study, a novel, patient-tailored approach was adopted to treat an elderly patient with relapsed metastatic NSCLC (mNSCLC), who was ineligible for targeted therapy (due to no suitable targeted drugs) and conventional chemotherapy (due to their age and poor physical condition). Specifically, multi-omics analysis for diagnosis, disease monitoring and guiding a dynamic treatment regime, including the final utilization of anti-PD-1/CIK cell combination therapy, was utilized for benefits in both disease control and health improvement. The present case describes an example of the integration of modern multi-omics technologies for better therapeutic approaches and clinical benefits in elderly patients with relapsed mNSCLC.

Case report

An 86-year-old female patient was admitted in May 2019 to the Elderly Respiratory Department, Henan Provincial People's Hospital (Zhengzhou, China) due to coughing up bloody sputum for ~2 weeks. They were then subjected to a set of multi-omics analyses, including next-generation sequencing (NGS)-based actionable gene panel sequencing, immunohistochemistry (IHC) for PD-L1, circulating tumor cell (CTC) assay and flow cytometric analysis of lymphocyte subsets (immune status) (Fig. 1). Conventional diagnostic methods for cancer, including pathological analysis of tumor biopsy and chest computed tomography (CT) were performed. In addition, routine examinations, including blood tests, urine tests, tumor biomarker detection, liver and kidney function tests, and an electrocardiogram, were performed. Based on preliminary diagnostic results, the patient was diagnosed with a relapsed NSCLC at stage IV with multiple metastases. Using CT imaging, a tumor was observed near the pulmonary hilum in the lower lobe of the left lung (Fig. 2). In addition, multiple nodules in both lungs spreading into the right anterior chest and bilateral abdominal walls, thickened left adrenal gland, as well as the destruction of multiple bones in C3 and L4 vertebrae and the right sacral wing were observed. Increased plasma levels of tumor markers cancer antigen (CA)199 (63.39 U/ml; reference value 0-30 U/ml) and CA153 (34.12 U/ml; reference value 0-24 U/ml) were observed (Table I). Additionally, 15 CTCs (3 mesenchymal types and 12 hybrid types) were identified in peripheral blood (Fig. 3A-C); hematoxylin and eosin (H&E) staining showed both normal and tumor cells (Fig. 3D); IHC revealed a high content of cancer cells (80%) expressing PD-L1 (anti-PD-L1 antibody; monoclonal 22C3; Dako; Agilent Technologies, Inc.) (Fig. 3E). Moreover, flow cytometric analysis (Fig. 4) suggested T-cell immunodeficiency with decreased counts for lymphocytes (CD45⁺), total T cells (CD3⁺), T helper cells (CD3⁺CD4⁺), a decreased CD4⁺/CD8⁺ T-cell ratio, dysregulation of regulatory T (Treg)

cells (CD45⁺CD4⁺CD25⁺CD127^{dim/-}), and an increased number of activated T cells and NK cells (Table II, month 0). While NGS-based actionable gene sequencing (Burning Rock Biotech, Ltd.) detected no targetable mutations, with the exception of a KRAS mutation (c.35G>A, p.G12D). The patient also showed signs of poor health, including multiple underlying diseases (cerebral infarction, hypertension grade 3, hyperlipidemia, paroxysmal supraventricular tachycardia and age-related dementia with brain atrophy) and general conditions of ill health (pain, fatigue, malaise, a loss of appetite and poor mental state).

Informed by integrative results from these multi-omics analyses and the health condition of the patient, a patient-tailored treatment plan using PD-1 blockade immunotherapy (sintilimab; Innovent Biologics, Inc.; 200 mg each treatment every 3-4 weeks) was implemented, since PD-1 inhibitors have shown efficacy in treating patients with NSCLC (24,25). The response to treatment was also monitored periodically by examinations including routine follow-up examinations for cancer, CT, CTC analysis and flow cytometric analysis of immune status. The curative effect, including complete response (CR), partial response (PR), stable disease (SD) and progressive disease, was evaluated according to the Response Evaluation Criteria in Solid Tumors (version 1.1) guidelines (26). The adverse reactions were judged according to the World Health Organization grading standard (27) of acute and subacute adverse reactions of anticancer drugs, such as myelosuppression, digestive tract reaction, hypersensitivity, fever, neuropathy and phlebitis. After two courses of sintilimab treatment, SD was achieved; however, the symptoms, including cancer-associated pain, fatigue, malaise, a loss of appetite and poor mental state were not significantly improved. CIK cells have been suggested to improve the quality of life and enhance the effect of anti-PD-1 immunotherapy (28). Therefore, CIK cell infusions (1-2x10⁹ cells/day for 3 consecutive days in each session, once per month and ≥3 days away from the treatment of PD-1 blockade) were added in combination with sintilimab to the subsequent courses of treatment. After a total of four courses of combined PD-1/CIK therapy, remission without severe adverse events in the cancer and general condition of the patient was eventually achieved, including alleviation of pain, decreased malaise, and improvements in food intake and mental state. The diagnostic status of the patient significantly improved, including a CTC count of 0, normal serum levels of tumor biomarkers (Table I) and a significantly improved status for T-cell immunodeficiency (Table II, month 10). The patient did not require further treatment and continued to display an improved condition for the next 12 months until the end of the follow-up. These results demonstrated that the combination of CIK cell therapy with PD-1 blockade therapy significantly improved therapeutic efficacy, and multi-omics analysis for initial diagnosis and follow-up disease monitoring can be used to inform the selection of the appropriate regimen for an improved outcome. The treatment and testing procedures for this elderly patient with mNSCLC are summarized in Fig. 5.

The methods of the aforementioned multi-omics analysis were performed as follows. First, NGS was performed as described previously (29). This method employed targeted capture of exonic and partially intronic regions of eight genes

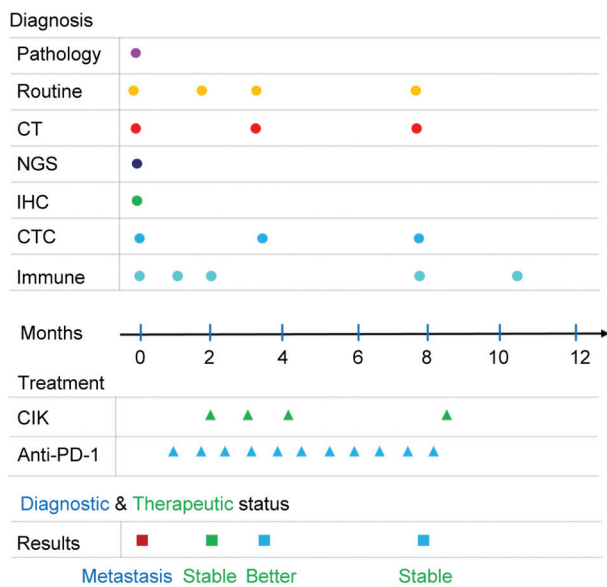


Figure 1. Time chart of the diagnosis, treatment and therapeutic outcomes of the patient during the entire process of disease management. Routine refers to routine inspection, including blood tests, urine tests, tumor biomarker detection, liver and kidney function tests, and an electrocardiogram. Immune refers to immune index detection via flow cytometric analysis of lymphocyte subsets. CT, computed tomography; IHC, immunohistochemistry; CTC, circulating tumor cell; CIK, cytokine-induced killer; NGS, next generation sequencing; PD-1, programmed death protein 1.

that are recommended by the National Comprehensive Cancer Network guidelines and are highly relevant to NSCLC personalized treatment regimens (30). The eight-gene panel covered oncogenic driver mutations of EGFR, ALK, BRAF, MET, RET, ROS1, ERBB2 and KRAS (now upgraded to a nine-gene panel Langke[®] CDx; NMPA certificate# 20223400343; Burning Rock Biotech, Ltd.). Tissue DNA was extracted from formalin-fixed, paraffin-embedded (FFPE) tumor tissue using a QIAamp DNA FFPE tissue kit (Qiagen GmbH) according to the manufacturer's instructions. DNA quantification was performed using a Qubit fluorescence quantitative analyzer (Invitrogen; Thermo Fisher Scientific, Inc.). Tissue DNA fragments between 200 and 400 bp were purified (Agencourt AMPure XP Kit; cat. no. A63881; Beckman Coulter, Inc.), hybridized with capture probe baits, selected with magnetic beads and amplified. Target capture was performed using a commercial panel consisting of 8 lung cancer-related genes (Burning Rock Biotech, Ltd.). The loading concentration of the final library was 1.6 pM for DNA sequencing. The quality and the size of the fragments were assessed using a high sensitivity DNA kit and Bioanalyzer 2100 (Agilent Technologies, Inc.). Indexed samples were sequenced on the NextSeq 550 sequencing system (Illumina, Inc.) using the NextSeq 500/550 kit (300 cycles; cat. no. 20024908; Illumina, Inc.) with paired-end reads and average sequencing depth of 1,000 x for tissue samples. Adapters were trimmed from the sequence data with Trimmomatic v0.39 (<http://www.usadellab.org/cms/index.php?page=trimmomatic>) and were assessed with FastQC v0.11.9 (<https://www.bioinformatics.babraham.ac.uk/projects/fastqc/>) to ensure the 'per base sequence quality' of the reads was >30 (Phred quality score). Subsequently, sequence reads were mapped to the human

Table I. Levels of blood cancer markers during the treatment process.

Blood cancer marker	Months after hospitalization			
	0	2	3	8
CEA (0-5 ng/ml)	2.89	2.54	1.27	3.09
AFP (0-7 ng/ml)	3.01	1.82	2.75	3.56
CA125 (0-25 U/ml)	20.96	20.01	19.15	14.21
CA199 (0-30 U/ml)	63.39 ^a	40.34 ^a	24.43	23.81
CA153 (0-24 U/ml)	34.12 ^a	29.78 ^a	17.23	19.28

^aHigher than normal range. Values in brackets refer to the normal range. CEA, carcinoembryonic antigen; AFP, α -fetoprotein; CA, cancer antigen.

genome (hg19) using the BWA aligner 0.7.10 (<http://maq.sourceforge.net>). Picard (<http://broadinstitute.github.io/picard/>) was utilized to mark and remove duplicates in the resultant alignment file. Local alignment optimization and variant calling were performed using Genome Analysis ToolKit 3.2 (http://www.broadinstitute.org/gsa/wiki/index.php/The_Genome_Analysis_Toolkit) and VarScan (<http://varscan.sourceforge.net>). Variants were filtered using the VarScan ffilter pipeline. At least five supporting reads were needed for insertion-deletions, while eight supporting reads were needed for single nucleotide variants to be called. According to the ExAC in gnomAD (<https://gnomad.broadinstitute.org/>), 1000 Genomes (<http://www.1000genomes.org>), dbSNP (<https://www.ncbi.nlm.nih.gov/SNP/>) and ESP6500SI-V2 (<https://esp.gs.washington.edu/drupal/>) databases, variants with a population frequency >0.1% were grouped as single nucleotide polymorphisms and excluded from further analysis. The remaining variants were annotated with ANNOVAR (<https://annovar.openbioinformatics.org/>) and SnpEff v3.6 (http://sourceforge.net/projects/snpeff/files/snpeff_latest_core.zip). DNA translocation analysis was performed using both Tophat 2 (<http://ccb.jhu.edu/software/tophat/index.shtml>) and Factera (<http://factera.stanford.edu>), and copy number variants were analyzed with CNVkit (<https://cnvkit.readthedocs.io/en/stable/>) (29).

Second, the characterization of CTCs was performed using the CanPatrol[®] System and Tricolor RNA-ISH method (certificate# 20142221528; Yishan Biotechnology Co., Ltd.) as described previously (31). Briefly, 5 ml peripheral blood was immediately collected and transferred to EDTA-coated tubes. To remove red blood cells, a lysis buffer (MilliporeSigma) was added. After 30 min, centrifugation (600 x g for 5 min at room temperature) was performed and the supernatant was removed. The remaining cells were further separated using a CanPatrol[®] CTC enrichment technique (Yishan Biotechnology Co., Ltd.). For the identification of different CTC subtypes, cells were incubated at 42°C for 2.5 h (ready to use according to the manufacturer's instructions) with the following probes (Yishan Biotechnology Co., Ltd.): Alexa Fluor 594-conjugated epithelial biomarkers epithelial cellular adhesion

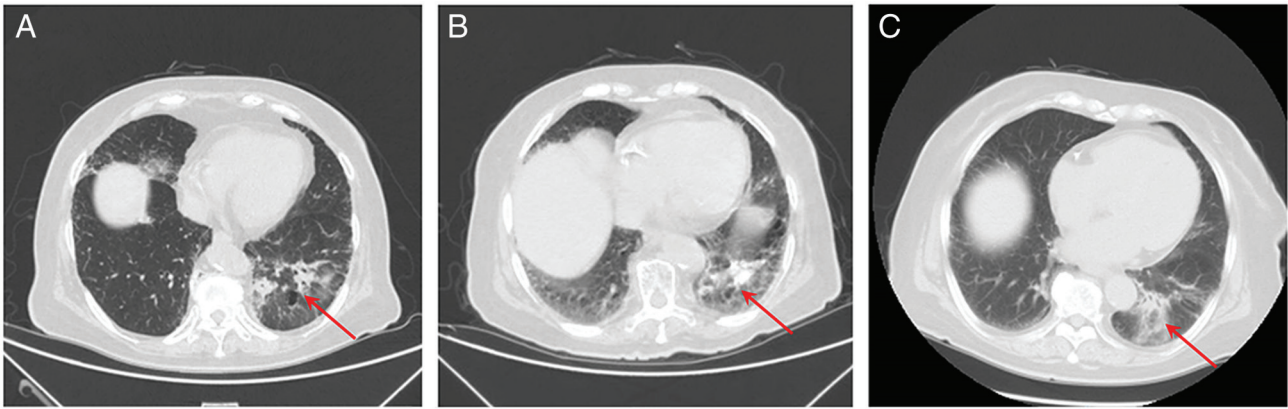


Figure 2. CT images during the treatment process. (A) A representative CT scan showed a tumor and a cavity near the pulmonary hilum in the lower lobe of the left lung (arrow) at the initial diagnosis. (B) After two rounds of PD-1 and CIK cell combined treatment, the CT scan showed improvement (arrow). (C) After 11 treatments with PD-1 and three treatments with CIK cells, the CT scan showed that the disease status was stable (arrow). CT, computed tomography; CIK, cytokine-induced killer; PD-1, programmed death protein 1.

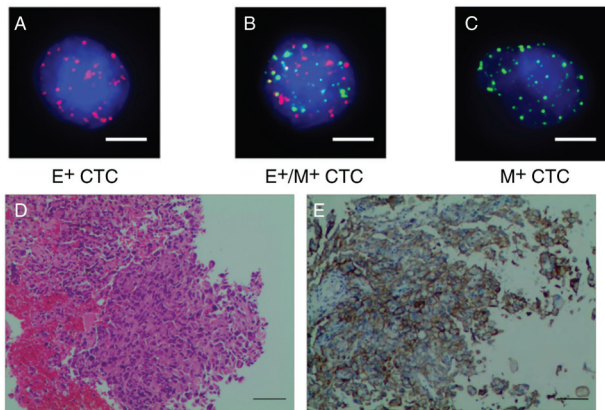


Figure 3. Representative images showing the results of CTC and immunohistochemistry analyses. (A-C) Epithelial-mesenchymal transition phenotype of CTCs, as determined by RNA in situ hybridization. The nuclei were stained with DAPI (blue); (A) E⁺ CTCs were stained with epithelial cell adhesion molecule and cytokeratin 8/18/19 markers (red dots); (B) E⁺/M⁺ CTCs contain both epithelial (red) and mesenchymal (green) markers; (C) M⁺ CTCs were stained with Vimentin and Twist markers (green dots). Scale bar, 5 μ m. Representative images of (D) hematoxylin and eosin staining, and (E) PD-L1 immunohistochemistry in tumor tissues (~80% of tumor cells were anti-PD-L1-positive). Scale bar, 100 μ m. CTC, circulating tumor cell; E⁺, epithelial; M⁺, mesenchymal; PD-L1, programmed death ligand 1.

molecule (EpCAM; cat. no. Su-KC0824), cytokeratin (CK)8 (cat. no. Su-KC0924), CK18 (cat. no. Su-KC1024) and CK19 (cat. no. Su-KC1124); Alexa Fluor 488-conjugated mesenchymal biomarkers Vimentin (cat. no. Su-KC1224) and Twist (cat. no. Su-KC1324); and Alexa Fluor 647-conjugated leukocyte biomarker CD45 (cat. no. Su-KC0724); and the nuclei were stained with DAPI (MilliporeSigma). After staining with DAPI (MilliporeSigma) for 30 min at 4°C, the cells were washed with 2% goat serum PBS (MilliporeSigma) solution and images were captured at x400 magnification using an Axio Imager Z2 fluorescence microscope (Carl Zeiss AG).

Third, lymphocyte subset measurements using flow cytometry were performed as described in detail previously (32). Briefly, peripheral blood mononuclear cells (PBMCs) were

isolated by Ficoll 400 density gradient liquid (Cytiva) centrifugation for 30 min at 600 x g and room temperature, blocked for 15 min at 4°C with FcR (BD Pharmingen; BD Biosciences) and incubated with BD Horizon™ Fixable Viability Stain 575V (cat. no. 565694; BD Horizon; BD Biosciences) for 15 min at room temperature. Cells were then washed twice with fluorescence-activated cell sorter (FACS) buffer (BD Pharmingen; BD Biosciences). For surface marker staining, BD Multitest™ 6-Color TBNK (cat. no. 662967; BD Pharmingen; BD Biosciences), including anti-human CD45-PerCP-Cy5.5, CD3-FITC, CD4-PE-Cy7, CD8-APC-Cy7, CD19-APC and CD16+CD56-PE antibodies for the T/B/NK lymphocyte subset; CD45-PerCP-Cy5.5 (cat. no. 340952; BD Pharmingen; BD Biosciences), CD4-FITC (cat. no. 340133; BD Pharmingen; BD Biosciences), CD25-PE (cat. no. 341010; BD Pharmingen; BD Biosciences) and CD127-APC (cat. no. Z6410052; Beijing Tongsheng Shidai Biotech Co., Ltd.) antibodies for Treg cells; CD45-PerCP (cat. no. 340665; BD Pharmingen; BD Biosciences), CD3-PE (cat. no. 340662; BD Pharmingen; BD Biosciences), CD5-APC (cat. no. 340658; BD Pharmingen; BD Biosciences), CD19-V450 (cat. no. 644492; BD Horizon; BD Biosciences) and HLA-DR-V500 (cat. no. 561224; BD Horizon; BD Biosciences) antibodies for B1/B2 cells and activated T cells were added to cells at the recommended doses (ready to use), and incubated for 20 min at room temperature. The cells were then washed twice with FACS buffer. Cell analysis was performed using a FACS machine (BD FACSCantoII; BD Biosciences) and cell populations were analyzed using BD FACSDiva software v8.0.1 (BD Biosciences; Fig. 4).

Finally, IHC was performed as described previously (33). Briefly, the NSCLC tissue (collected May 2019) was fixed in 10% neutral fixative at room temperature for 3-4 h. An appropriately sized tissue section was placed into an embedding box for dehydration. The dehydrated tissue was then embedded in paraffin and sectioned with a microtome into 3- μ m slices, which were subjected to immunohistochemical staining using the PD-L1 IHC 22C3 pharmDx kit (cat. no. SK006; Dako; Agilent Technologies, Inc.) on the Dako Autostainer Link 48 platform (Dako; Agilent Technologies, Inc.). The paraffin-embedded sections were dewaxed and

Table II. Immune status monitored by flow cytometric analysis of lymphocyte subsets during the treatment process.

Lymphocyte subset	Months after hospitalization				
	0	1	2	8	10
Lymphocyte (CD45 ⁺) (20-50%)	16.50% ^a	16.40% ^a	21.50% ^b	35.60% ^b	33.30% ^b
T cell (CD3 ⁺) (55.62-84.84%)	54.60% ^a	54.80% ^a	59.10% ^b	39.90% ^a	57.40% ^b
B cell (CD19 ⁺) (6.58-24.52%)	12.90% ^b	5.90% ^a	8.50% ^b	9.30% ^b	19.10% ^b
Th cell (CD3 ⁺ CD4 ⁺) (31.07-60.03%)	24.40% ^a	26.80% ^a	34.40% ^b	14.30% ^a	35.90% ^b
Tc cell (CD3 ⁺ CD8 ⁺) (13.27-40.63%)	25.10% ^b	23.00% ^b	21.60% ^b	23.60% ^b	19.90% ^b
NK cell (CD3 ⁻ /CD16 ⁺ CD56 ⁺) (5.15-27.08%)	30.80% ^c	36.30% ^c	30.10% ^c	48.30% ^c	20.70% ^b
Treg cell (CD45 ⁺ CD4 ⁺ CD25 ⁺ CD127 ^{dim/-}) (5-10%)	12.30% ^a	17.20% ^a	18.70% ^a	26.20% ^a	25.90% ^a
Activated T cell (CD3 ⁺ HLA-DR ⁺) (0.37-13.98%)	14.70% ^c	8.20% ^b	17.00% ^c	5.00% ^b	3.70% ^b
NKT cell (CD3 ⁺ /CD16 ⁺ CD56 ⁺) (5.3-8.1%)	6.90% ^b	8.90% ^c	5.40% ^b	4.80% ^a	3.30% ^a
CD4/CD8 (ratio 1.4-2.47)	0.97 ^a	1.16 ^a	1.59 ^b	0.61 ^a	1.80 ^b
B1 CD19 ⁺ CD5 ⁺ (0-1.44%)	0.90% ^b	0.10% ^b	0.50% ^b	-	0.80% ^b
B2 CD19 ⁺ CD5 (4.74-16.74%)	13.30% ^b	5.00% ^b	7.70% ^b	-	10.00% ^b

^aChanges that promote cancer; ^bnormal values; ^cchanges that inhibit cancer. Values in brackets refer to the normal range; spaces indicate missing data. Th, helper T; Tc, cytotoxic T; NK, natural killer; NKT, natural killer T; Treg, regulatory T.

hydrated, and antigen retrieval was performed for 1 h at room temperature using the EnVision™ FLEX Target Retrieval Solution (Dako; Agilent Technologies, Inc.). After incubation with FLEX peroxidase non-specific binding blocking reagent (Dako; Agilent Technologies, Inc.) for 5 min at room temperature, the tissue was incubated with an anti-PD-L1 primary antibody (1:50; cat. no. M365329; Dako; Agilent Technologies, Inc.) for 60 min at room temperature, followed by incubation with the EnVision FLEX HRP visualization reagent (cat. no. SM802; ready to use; Dako; Agilent Technologies, Inc.) at room temperature for 30 min and color development using DAB chromogenic solution at room temperature for 10 min. The tissue was then counterstained with hematoxylin at room temperature for 2 min and a coverslip was added. All of the aforementioned steps were followed by washes in EnVision FLEX Wash Buffer 20X (1:20; Dako; Agilent Technologies, Inc.) for 5 min at room temperature.

H&E staining was also conducted on deparaffinized and rehydrated sections. The tissue was incubated with hematoxylin aqueous solution (Baso Diagnostic, Inc.) for 5 min at room temperature, differentiated in hydrochloric acid-ethanol differentiation solution, rinsed and then incubated with eosin staining solution (Baso Diagnostic, Inc.) for 3 min at room temperature. After dehydration with alcohol, clearing with xylene and sealing with a neutral resin, sections that underwent IHC and H&E staining were examined under a light microscope (x200 magnification).

Discussion

With advances in medicine, novel therapies, including targeted therapy, immunotherapy, CAR-T cell therapy and vaccines, have been developed for various types of cancer in the last few decades (34). This progress requires an improvement in

the development of diagnostic methodologies that can be used to inform therapy (35). Notably, it is difficult to treat elderly patients with R/R mNSCLC, especially when no targeted therapies are available due to a lack of targeted mutations (5). In the present case report, it was demonstrated that an elderly patient benefited from the integrative utilization of multi-omics analysis and dynamic treatment regimens. Based on the diagnostic results, PD-1 blockade alone was initially used to treat the patient, since it is a well-established treatment option for patients with NSCLC, particularly those with high levels of PD-L1 expression. At first, autologous CIK cell infusion was not performed, as it is expensive and requires time to manufacture. However, as informed by periodical monitoring of the response to treatment, a combination therapy of PD-1 blockade and infusion of autologous CIK cells was finally adopted, and the addition of CIK cells resulted in a significant improvement not only in the management of the patient's cancer but also in their general health. Notably, anti-PD-1/CIK cell combination therapy also induced significant clinical benefits in three other published studies, including 3 patients with CR, 3 patients with PR and 5 patients with SD, out of a total of 15 patients with NSCLC (16-18).

The precise mechanisms underlying PD-1/CIK combination therapy remain to be defined. Accumulating evidence has demonstrated that blocking the PD-1/PD-L1 pathway is an effective treatment option for multiple types of cancer, likely through the restoration of tumor-specific immune activity, since tumor cells may overexpress PD-L1 to co-opt the PD-1 pathway and to enable evasion of the immune response (36). It has been shown that the tumor regression achieved by anti-PD-1/PD-L1 drugs requires pre-existing T cells within the tumor microenvironment, which have been negatively regulated to confer tumor-mediated adaptive immune resistance (37-39). Furthermore, evidence has suggested that CIK cells, as a group of heterogeneous immune-active effector

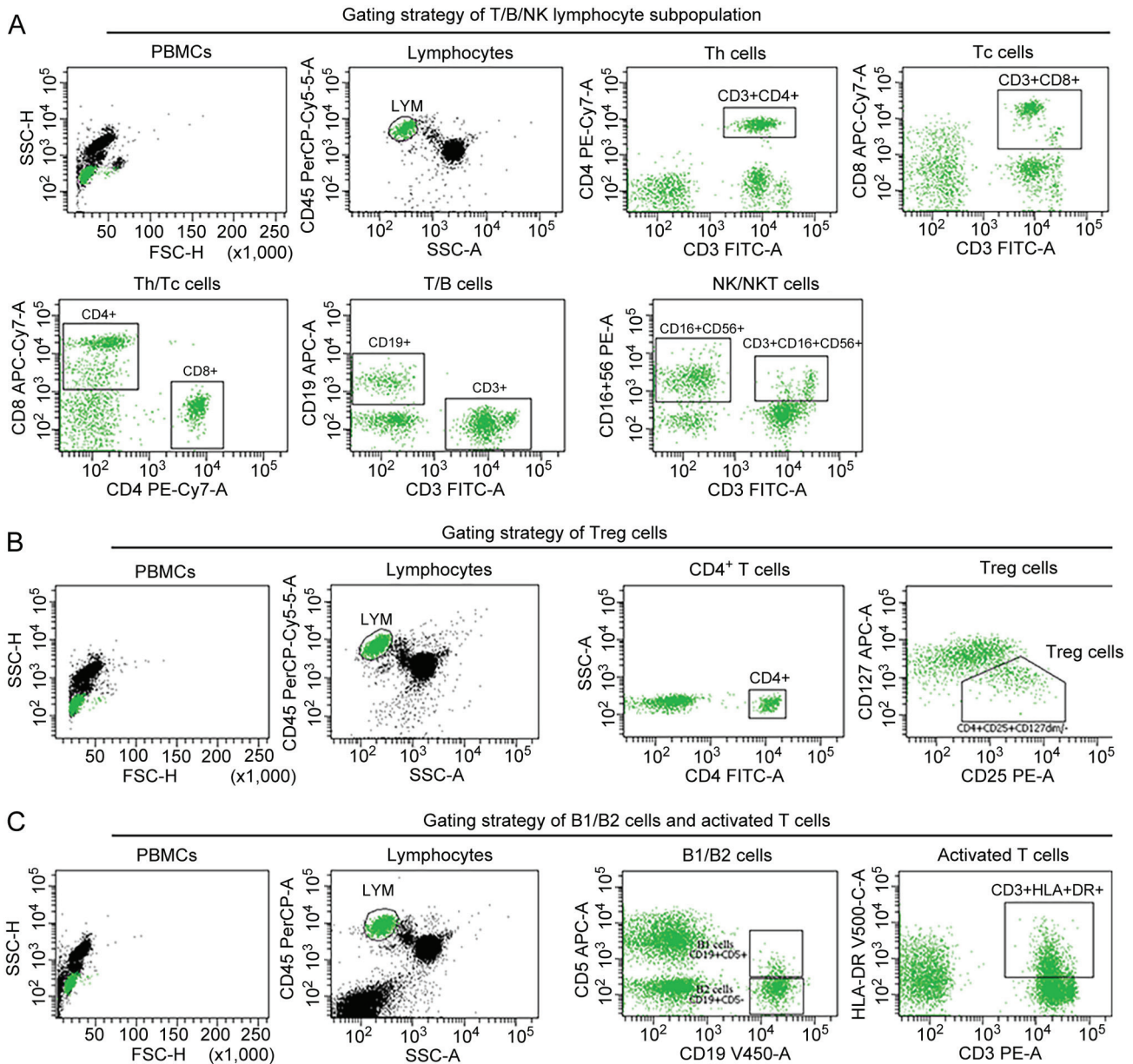


Figure 4. Assessment of peripheral blood immune status in the reported patient with metastatic NSCLC. PBMCs collected from the patient with NSCLC (month 0) were analyzed by flow cytometry for the percentage of (A) T/B/NK, (B) Treg and (C) B1/B2 and activated T cells. NSCLC, non-small cell lung cancer; PBMCs, peripheral blood mononuclear cells; Th, helper T; Tc, cytotoxic T; NK, natural killer; NKT, natural killer T; Treg, regulatory T.

cells, with the dual properties of both cytotoxic T lymphocytes and NK cells (19), can promote the efficacy of checkpoint inhibition involving PD-1 or other immune checkpoints (12). Conversely, *in vitro* studies have revealed that PD-1 blockade can also directly enhance the cytotoxicity of CIK cells (13-15). Therefore, it is likely that PD-1 blockade and CIK cell application can potentiate each other to synergistically enhance the therapeutic effect.

In the present case report, an example of the use of multi-omics analysis in assisting the selection of an optimal treatment plan is described. In this case, through integrating the results of multi-omics analysis and the continued monitoring of the response to treatment, dynamic therapeutic strategies were employed, including the use of PD-1 blockade and CIK cell infusion combination therapy, leading to significantly improved outcomes. Therefore, the present study is

informative as it is the first, to the best of our knowledge, to describe an effective treatment strategy for elderly patients who are usually unsuitable for most treatment options. In addition, the present study demonstrated the importance and benefit of a multi-omics approach for successful cancer management. However, the present study has some limitations; in particular, only one patient was reported on in the present case report. Therefore, further studies should be performed to validate this finding and to uncover the underlying mechanisms.

In conclusion, the present case report demonstrated that a multi-omics analysis approach can inform patient-tailored therapy to improve clinical outcomes in a hard-to-treat elderly patient with mNSCLC physically unsuitable for surgery and most types of chemotherapy, and genetically unsuitable for targeted therapy.

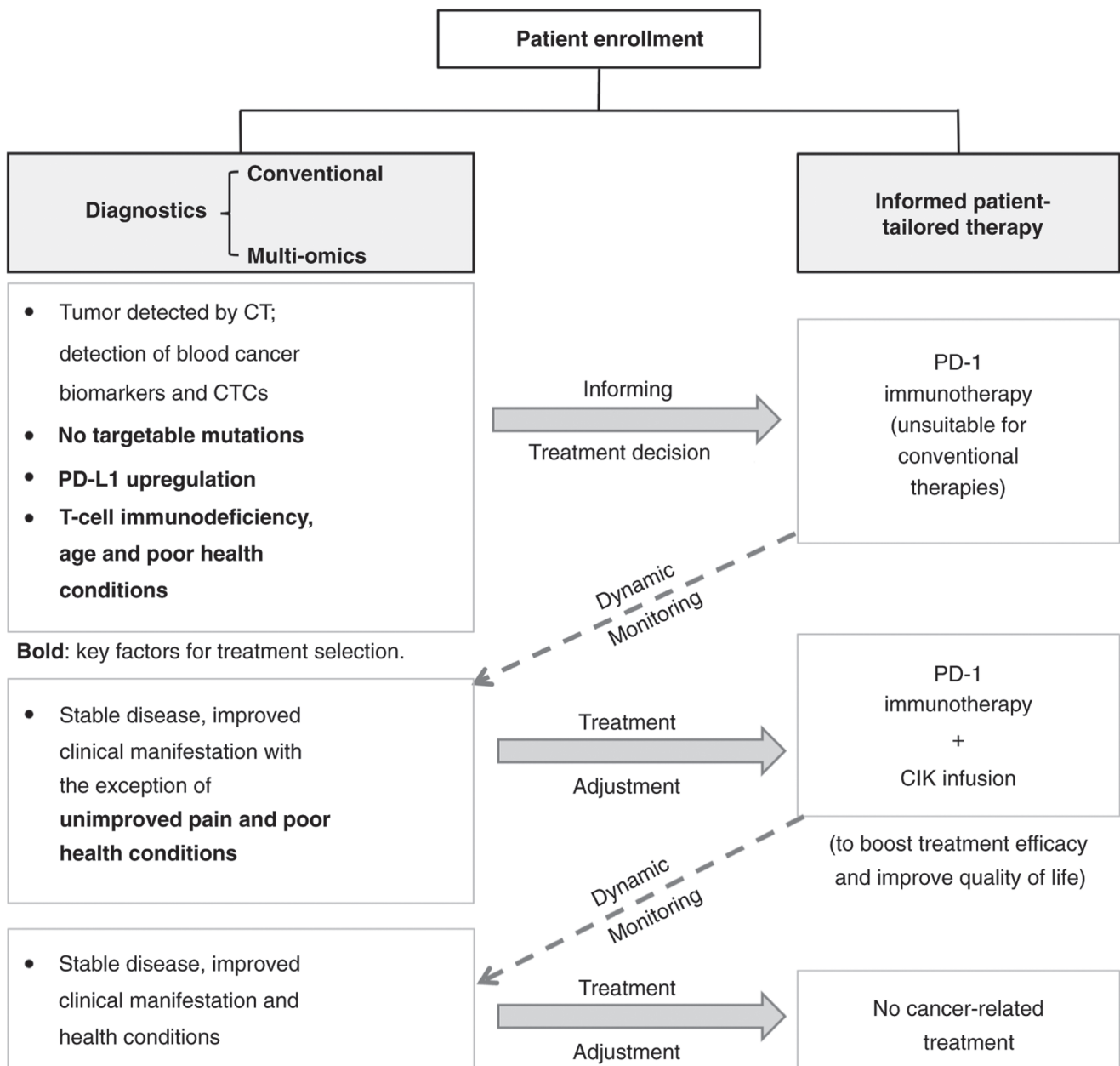


Figure 5. Schematic diagram of the treatment and testing procedures for the patient with metastatic non-small cell lung cancer. Upon admission, the patient was assessed using conventional and multi-omics diagnostic approaches, informing subsequent treatment selection using PD-1 blockade. The response to the treatment was monitored using the same diagnostic approaches and treatment adjustments were made accordingly until the desired outcome was achieved. CT, computed tomography; CTCs, circulating tumor cells; PD-L1, programmed death ligand 1; PD-1, programmed death protein 1; CIK, cytokine-induced killer.

Acknowledgements

Not applicable.

Funding

No funding was received.

Availability of data and materials

The NGS data generated in the present study may be found in the NCBI SRA database under the accession number SRR27406315 or at the following URL: <https://www.ncbi.nlm.nih.gov/sra/?term=SRR27406315>. All of the other data

generated in the present study may be requested from the corresponding author.

Authors' contributions

YX contributed to statistical analysis, wrote the original draft and assessed study quality. FQ, LH, JY and HZ contributed to indicator detection, data extraction and literature searching. YQ contributed to the establishment of a clinical treatment plan, evaluation of efficacy and data extraction. ST and YZ contributed to statistical analysis, and reviewed and edited the manuscript. YX and YZ confirm the authenticity of all the raw data. All authors contributed to the article, and have read and approved the final manuscript.

Ethics approval and consent to participate

Not applicable.

Patient consent for publication

The patient provided written informed consent for the publication of their data.

Competing interests

The authors declare that they have no competing interests.

References

- Chen W, Zheng R, Baade PD, Zhang S, Zeng H, Bray F, Jemal A, Yu XQ and He J: Cancer statistics in China, 2015. *CA Cancer J Clin* 66: 115-132, 2016.
- Ferlay J, Colombet M, Soerjomataram I, Parkin DM, Piñeros M, Znaor A and Bray F: Cancer statistics for the year 2020: An overview. *Int J Cancer* 149: 778-789, 2021.
- Sosa E, D'Souza G, Akhtar A, Sur M, Love K, Duffels J, Raz DJ, Kim JY, Sun V and Erhunmwunsee L: Racial and socioeconomic disparities in lung cancer screening in the United States: A systematic review. *CA Cancer J Clin* 71: 299-314, 2021.
- Khanna P, Blais N, Gaudreau PO and Corrales-Rodriguez L: Immunotherapy comes of age in lung cancer. *Clin Lung Cancer* 18: 13-22, 2017.
- Spagnuolo A and Gridelli C: The role of immunotherapy in the first-line treatment of elderly advanced non-small cell lung cancer. *Cancers (Basel)* 15: 2319, 2023.
- Xia L, Liu Y and Wang Y: PD-1/PD-L1 blockade therapy in advanced non-small-cell lung cancer: Current status and future directions. *Oncologist* 24 (Suppl 1): S31-S41, 2019.
- Momotow J, Bühnen I, Trautmann-Grill K, Kobbe G, Hahn D, Schroers R, Heinrich B, Gaska T, Forstbauer H, Schmidt B, *et al.*: Outcomes of anti-programmed death 1 treatment for relapsed/refractory Hodgkin lymphoma: A German Hodgkin Study Group multicentre real-world analysis. *Br J Haematol* 198: 401-404, 2022.
- Pan D, Hu AY, Antonia SJ and Li CY: A Gene mutation signature predicting immunotherapy benefits in patients with NSCLC. *J Thorac Oncol* 16: 419-427, 2021.
- Hoffner B, Leighl NB and Davies M: Toxicity management with combination chemotherapy and programmed death 1/programmed death ligand 1 inhibitor therapy in advanced lung cancer. *Cancer Treat Rev* 85: 101979, 2020.
- Yi M, Zheng X, Niu M, Zhu S, Ge H and Wu K: Combination strategies with PD-1/PD-L1 blockade: Current advances and future directions. *Mol Cancer* 21: 28, 2022.
- Huang K, Sun B, Luo N, Guo H, Hu J and Peng J: Programmed death receptor 1 (PD1) knockout and human telomerase reverse transcriptase (hTERT) transduction can enhance persistence and antitumor efficacy of cytokine-induced killer cells against hepatocellular carcinoma. *Med Sci Monit* 24: 4573-4582, 2018.
- Dehno MN, Li Y, Weiher H and Schmidt-Wolf IGH: Increase in efficacy of checkpoint inhibition by cytokine-induced-killer cells as a combination immunotherapy for renal cancer. *Int J Mol Sci* 21: 3078, 2020.
- Chen J, Chen Y, Feng F, Chen C, Zeng H, Wen S, Xu X, He J and Li J: Programmed cell death protein-1/programmed death-ligand 1 blockade enhances the antitumor efficacy of adoptive cell therapy against non-small cell lung cancer. *J Thorac Dis* 10: 6711-6721, 2018.
- Poh SL and Linn YC: Immune checkpoint inhibitors enhance cytotoxicity of cytokine-induced killer cells against human myeloid leukaemic blasts. *Cancer Immunol Immunother* 65: 525-536, 2016.
- Liu LW, Yang MY, Zhou M, Li JJ, Liu B and Pan YY: Improvement of cytotoxicity of autologous CIKs from patients with breast cancer to MCF-7 cells by suppressed PD-1 expression. *Cancer Biomark* 20: 609-615, 2017.
- Han Y, Mu D, Liu T, Zhang H, Zhang J, Li S, Wang R, Du W, Hui Z, Zhang X and Ren X: Autologous cytokine-induced killer (CIK) cells enhance the clinical response to PD-1 blocking antibodies in patients with advanced non-small cell lung cancer: A preliminary study. *Thorac Cancer* 12: 145-152, 2021.
- Wang Z, Liu X, Till B, Sun M, Li X and Gao Q: Combination of cytokine-induced killer cells and programmed cell death-1 blockade works synergistically to enhance therapeutic efficacy in metastatic renal cell carcinoma and non-small cell lung cancer. *Front Immunol* 9: 1513, 2018.
- Zhao L, Han L, Zhang Y, Li T, Yang Y, Li W, Shang Y, Lin H and Gao Q: Combination of PD-1 blockade and RetroNectin[®]-activated cytokine-induced killer in preheavily treated non-small-cell lung cancer: A retrospective study. *Immunotherapy* 10: 1315-1323, 2018.
- Pievani A, Borleri G, Pende D, Moretta L, Rambaldi A, Golay J and Introna M: Dual-functional capability of CD3+CD56+ CIK cells, a T-cell subset that acquires NK function and retains TCR-mediated specific cytotoxicity. *Blood* 118: 3301-3310, 2011.
- Mata-Molanes JJ, Sureda González M, Valenzuela Jiménez B, Martínez Navarro EM and Brugarolas Maslllorens A: Cancer immunotherapy with cytokine-induced killer cells. *Target Oncol* 12: 289-299, 2017.
- Zhang X, Huang H, Han L, Li T, Wang Z and Gao Q: Advanced renal-cell carcinoma pseudoprogression after combined immunotherapy: Case report and literature review. *Front Oncol* 11: 640447, 2021.
- Zhao L, Li T, Song Y, Yang Y, Ma B, Zhang Y, Shang Y, Xu B, Guo J, Qin P, *et al.*: High complete response rate in patients with metastatic renal cell carcinoma receiving autologous cytokine-induced killer cell therapy plus anti-programmed death-1 agent: A single-center study. *Front Immunol* 12: 779248, 2022.
- Sharma A and Schmidt-Wolf IGH: 30 Years of CIK cell therapy: Recapitulating the key breakthroughs and future perspective. *J Exp Clin Cancer Res* 40: 388, 2021.
- Gao S, Li N, Gao S, Xue Q, Ying J, Wang S, Tao X, Zhao J, Mao Y, Wang B, *et al.*: Neoadjuvant PD-1 inhibitor (Sintilimab) in NSCLC. *J Thorac Oncol* 15: 816-826, 2020.
- Zhang F, Guo W, Zhou B, Wang S, Li N, Qiu B, Lv F, Zhao L, Li J, Shao K, *et al.*: Three-year follow-up of neoadjuvant programmed cell death protein-1 inhibitor (Sintilimab) in NSCLC. *J Thorac Oncol* 17: 909-920, 2022.
- Eisenhauer EA, Therasse P, Bogaerts J, Schwartz LH, Sargent D, Ford R, Dancey J, Arbuck S, Gwyther S, Mooney M, *et al.*: New response evaluation criteria in solid tumours: Revised RECIST guideline (version 1.1). *Eur J Cancer* 45: 228-247, 2009.
- Helling M and Venulet J: Drug recording and classification by the WHO research centre for international monitoring of adverse reactions to drugs. *Methods Inf Med* 13: 169-178, 1974.
- Vaseq R, Sharma A, Li Y and Schmidt-Wolf IGH: Revising the landscape of cytokine-induced killer cell therapy in lung cancer: Focus on immune checkpoint inhibitors. *Int J Mol Sci* 24: 5626, 2023.
- Feng Y, Feng G, Lu X, Qian W, Ye J, Manrique CA, Ma C and Lu Y: written on behalf of the AME Lung Cancer Collaborative Group: Exploratory analysis of introducing next-generation sequencing-based method to treatment-naïve lung cancer patients. *J Thorac Dis* 10: 5904-5912, 2018.
- Tsoulos N, Papadopoulou E, Metaxa-Mariatou V, Tsaousis G, Efstathiadou C, Tounta G, Skapeti K, Bourkoula J, Zarogoulidis P, Pentheroudakis GE, *et al.*: Molecular profiling of 502 patient cohort with NSCLC using a 27 somatic gene panel. *J Clin Oncol* 35: e23193, 2017.
- Xing Y, Qin F, Zhai Y, Yang J, Yan Y, Li D, Zhang H, Hu R, Xu X, Cao X, *et al.*: Association of clinical features of colorectal cancer with circulating tumor cells and systemic inflammatory markers. *Dis Markers* 2022: 5105599, 2022.
- Xing Y, Zhang X, Qin F, Yang J, Ai L, Wang Q and Zhai Y: The clinical significance of circulating tumor cells and T lymphocyte subtypes in pancreatic cancer patients. *Bioengineered* 13: 2130-2138, 2022.
- Yang X, Jiang L, Jin Y, Li P, Hou Y, Yun J, Wu C, Sun W, Fan X, Kuang D, *et al.*: PD-L1 expression in chinese patients with advanced non-small cell lung cancer (NSCLC): A multi-center retrospective observational study. *J Cancer* 24: 7390-7398, 2021.

34. Poondla N, Sheykhasan M, Akbari M, Samadi P, Kalhor N and Manoochehri H: The promise of CAR T-cell therapy for the treatment of cancer stem cells: A short review. *Curr Stem Cell Res Ther* 17: 400-406, 2022.
35. Tang Q, Zuo W, Wan C, Xiong S, Xu C, Yuan C, Sun Q, Zhou L and Li X: Comprehensive genomic profiling of upper tract urothelial carcinoma and urothelial carcinoma of the bladder identifies distinct molecular characterizations with potential implications for targeted therapy & immunotherapy. *Front Immunol* 13: 1097730, 2023.
36. Weber J: Immune checkpoint proteins: A new therapeutic paradigm for cancer-preclinical background: CTLA-4 and PD-1 blockade. *Semin Oncol* 37: 430-439, 2010.
37. Powles T, Eder JP, Fine GD, Braiteh FS, Loriot Y, Cruz C, Bellmunt J, Burris HA, Petrylak DP, Teng SL, *et al*: MPDL3280A (anti-PD-L1) treatment leads to clinical activity in metastatic bladder cancer. *Nature* 515: 558-562, 2014.
38. Herbst RS, Soria JC, Kowanetz M, Fine GD, Hamid O, Gordon MS, Sosman JA, McDermott DF, Powderly JD, Gettinger SN, *et al*: Predictive correlates of response to the anti-PD-L1 antibody MPDL3280A in cancer patients. *Nature* 515: 563-567, 2014.
39. Tumei PC, Harview CL, Yearley JH, Shintaku IP, Taylor EJ, Robert L, Chmielowski B, Spasic M, Henry G, Ciobanu V, *et al*: PD-1 blockade induces responses by inhibiting adaptive immune resistance. *Nature* 515: 568-571, 2014.



Copyright © 2024 Xing et al. This work is licensed under a Creative Commons Attribution-NonCommercial-NoDerivatives 4.0 International (CC BY-NC-ND 4.0) License.